Effective potential in scalar field theory

Kerson Huang, Efstratios Manousakis, and Janos Polonyi*
Center for Theoretical Physics, Laboratory for Nuclear Science and Department of Physics, Massachusetts Institute of Technology, Cambridge, Massachusetts 02139
(Received 19 November 1986; revised manuscript received 5 January 1987)

We study the $\lambda\phi^4$ theory in 4 space-time dimensions in a Monte Carlo simulation on a 10^4 lattice, through an especially simple and accurate way to calculate the effective potential. All renormalized parameters are obtained via the effective potential and the propagator. In the continuum limit we confirm the vanishing of the renormalized self-coupling, and show that the system can exist in one of two possible phases, both having a free particle of arbitrary mass. In one phase the vacuum expectation of the field vanishes, while in the other it is nonzero. This opens the possibility that, even though the self-coupling vanishes, the field can still be used to generate masses for gauge bosons and fermions.

I. INTRODUCTION

Ever since Wilson[1] showed that in 4 space-time dimensions the self-coupling of the $\lambda\phi^4$ theory vanishes, there has been extensive analytic and numerical study on the subject.[2,3] The interest is justified by the importance of understanding this simplest of all quantum field theories, as a prelude to studying the Higgs sector in the standard model, and in grand unified theories. We offer some new insight to the problem gained through a Monte Carlo calculation of the effective potential.

Consider a one-component scalar field $\phi(x)$ in an external source $J(x)$, with classical Lagrangian density in Minkowski space given by

$$L(x)=\tfrac{1}{2}(\partial\phi)^2-\tfrac{1}{2}r_0\phi^2-\tfrac{1}{4}\lambda_0\phi^4+J\phi\ , \tag{1}$$

where $\lambda_0>0$ and $-\infty<r_0<\infty$. The quantum theory is defined through the usual Euclidean path integral. An ultraviolet cutoff is introduced by discretizing Euclidean space-time as a four-dimensional (4D) square lattice of spacing a. Eventually the cutoff is removed by taking the continuum limit $a\to 0$, with the usual attendant renormalizations. The field ϕ and the mass gap m (invariant mass of the lowest excited state) both have dimensions of inverse length, and hence have the forms

$$\phi=a^{-1}\phi_{\text{latt}},\quad m=a^{-1}m_{\text{latt}}\ , \tag{2}$$

where ϕ_{latt} is a dimensionless field (but still unrenormalized) and m_{latt} is a dimensionless mass (renormalized). The renormalized field is $\phi_r=Z^{-1/2}\phi$, where Z is the wave-function renormalization constant. Correspondingly $Z^{-1/2}\phi_{\text{latt}}$ is the dimensionless renormalized field. Clearly both m_{latt} and ϕ_{latt} must vanish in the continuum limit, but the parameter

$$b=\langle\phi_r\rangle/m=Z^{-1/2}\langle\phi_{\text{latt}}\rangle/m_{\text{latt}} \tag{3}$$

may be nonzero and finite. At fixed λ_0 the continuum limit corresponds to the critical value of r_0 at which $m_{\text{latt}}=0$. On both sides of this critical point we expect to find different phases, which correspond to continuum field theories with or without spontaneous symmetry breaking (i.e., the parameter b defined above is nonzero in one phase, but vanishes in the other). The critical value of r_0 is generally nonzero; it vanishes only in lowest-order perturbation theory.

The mass m_{latt} can be extracted from the two-particle correlation function, or propagator $\Delta(x)$, as follows. We integrate $\Delta(x)$ over spatial coordinates at large values of the Euclidean time x_4. The result should be proportional to $\exp(-mx_4)$. Setting $x_4=a\tau$, so that τ is dimensionless, we have $mx_4=m_{\text{latt}}\tau$. The wave-function renormalization constant Z may be extracted from the Fourier transform $\tilde{\Delta}(p)$ of $\Delta(x)$, as the residue of the pole at $p^2=m^2$. Defining $\tilde{\Delta}_{\text{latt}}(p)=a^{-2}\tilde{\Delta}(p)$, we can write

$$Z=\lim_{a\to 0}\,[m_{\text{latt}}{}^2\tilde{\Delta}_{\text{latt}}(0)]\ . \tag{4}$$

Our renormalized self-coupling constant λ_r is defined as $\frac{1}{6}$ of the amputated one-particle-irreducible (1PI) 4-point function at zero momenta. (The factor $\frac{1}{6}$ is chosen so that in lowest-order perturbation theory $\lambda_r=\lambda_0$.) In numerical calculations, we can get better accuracies by extracting it from the effective potential $U(\phi)$, which can be calculated as follows.[4] Introduce a constant external source J, and calculate the vacuum expectation $f=\langle\phi\rangle$. By regarding J as a function of f we have the derivative of the effective potential:

$$U'(f)=J(f)\ . \tag{5}$$

Let ϕ_0 be the vacuum expectation of the field in the absence of an external source, i.e., $J(\phi_0)=0$. The effective potential has the following expansion:

$$U(\phi)=\sum_{n=2}^{\infty}\frac{G^{(n)}}{n!}(\phi-\phi_0)^n\ , \tag{6}$$

where $G^{(n)}$ is the Fourier transform of the unrenormalized amputated 1PI n-point function, with all external four-momenta set to zero. The renormalized version of $G^{(n)}$ is

$$G_r^{(n)}=Z^{n/2}G^{(n)}\ , \tag{7}$$

where the wave-function renormalization constant Z can be obtained from (4) by noting that

$$J'(\phi_0)=[\tilde{\Delta}_{\rm latt}(0)]^{-1} . \tag{8}$$

Thus we can obtain the following renormalized parameters from $J(f)$:

$$\lambda_r=Z^2 J'''(\phi_0) , \tag{9}$$

$$\lambda_{3,r}=Z^{3/2} J''(\phi_0) , \tag{10}$$

$$m_{\rm latt}{}^2=ZJ'(\phi_0) . \tag{11}$$

Here λ_r is the renormalized four-particle vertex, and $\lambda_{3,r}$ the renormalized three-particle vertex, which is expected to be present when $\phi_0 \neq 0$. The relation (11) can be used as a check on $m_{\rm latt}$.

From the results of Ref. 2 we can deduce that a continuum limit does not exist for any $\lambda_r > 0$. The reason is that λ_0 becomes divergent at a nonzero lattice constant. This phenomenon is reminiscent of the exactly soluble Lee model,[5] in which a ghost[6] (bound state with negative norm) appears for all nonzero real values of the renormalized coupling constant. In fact, perturbation theory extended by the renormalization group[7] gives a result very similar to that in the Lee model:

$$\frac{1}{\lambda_0}=\frac{1}{\lambda_r}-\frac{3}{128\pi}\ln\left[\frac{\Lambda^2}{m^2}\right] , \tag{12}$$

where Λ is the cutoff momentum and m is a mass scale. For a fixed $\lambda_r > 0$ the cutoff is bounded by a critical value Λ_c, at which λ_0 diverges:

$$(\Lambda_c/m)^2=\exp(128\pi^2/3\lambda_r) . \tag{13}$$

Thus the cutoff can approach infinity only if $\lambda_r \to 0$. We call Λ_c the "ghost point," by analogy with the Lee model. The same phenomenon has been conjectured in quantum electrodynamics (the Landau ghost),[7] for which $\Lambda_c=m_e\exp(3\pi/\alpha)$, where m_e is the electron mass and α the fine-structure constant. As we shall see, however, perturbation theory vastly overestimates the value of Λ_c.

The divergence of λ_0 at the ghost point means that our theory reduces to a 4D Ising model, whose critical behavior therefore governs the continuum limit. Thus, the order parameter and the inverse correlation length have the behavior

$$\langle\phi_r\rangle \to t^{\beta}, \quad m \to t^{\nu} , \tag{14}$$

where $t=|r_0-r_c|$, r_c being the critical value of r_0. We can now verify that $b \to t^{\beta-\nu}=$const (up to possible logarithmic corrections) because in four dimensions the critical indices have the mean-field values $\beta=\nu=\frac{1}{2}$.

The relation (12) indicates that the ghost arises from the fact that the theory is not asymptotically free. From a more elementary point of view we can qualitatively understand the vanishing of λ_r in the continuum limit by appealing to the nonrelativistic analog of the system, which is an N-particle system with repulsive δ-function interactions. It is well known that such an interaction in the Schrödinger equation in three spatial dimensions does not lead to scattering; i.e., the T matrix is identically zero.

II. METHOD OF CALCULATION

We make Monte Carlo simulations of the field theory on a 10^4 square lattice with periodic boundary conditions. To update a site, we first flip the sign of ϕ with a probability determined by a "heat bath" algorithm, then increment it by a random number D, with $|D| < D_0$. The change is accepted or rejected according to a standard Metropolis algorithm. The value of D_0 is adjusted to give roughly a 50% acceptance rate. The purpose of the sign flip is to prevent the value of ϕ from being trapped in the neighborhood of one of two possible potential minima. For a fixed value of λ_0 we search for the critical point by varying r_0. For each λ_0 and r_0, the following quantities are calculated: (a) the propagator with $J=0$, which gives the wave-function renormalization Z and the mass gap $m_{\rm latt}$; (b) the ensemble average $f=\langle\phi_{\rm latt}\rangle$ for a range of values of J, which yields $J(f)$ as the derivative of the effective potential. We fit $J(f)$ to a least-squares polynomial in order to extract $m_{\rm latt}$ and λ_r.

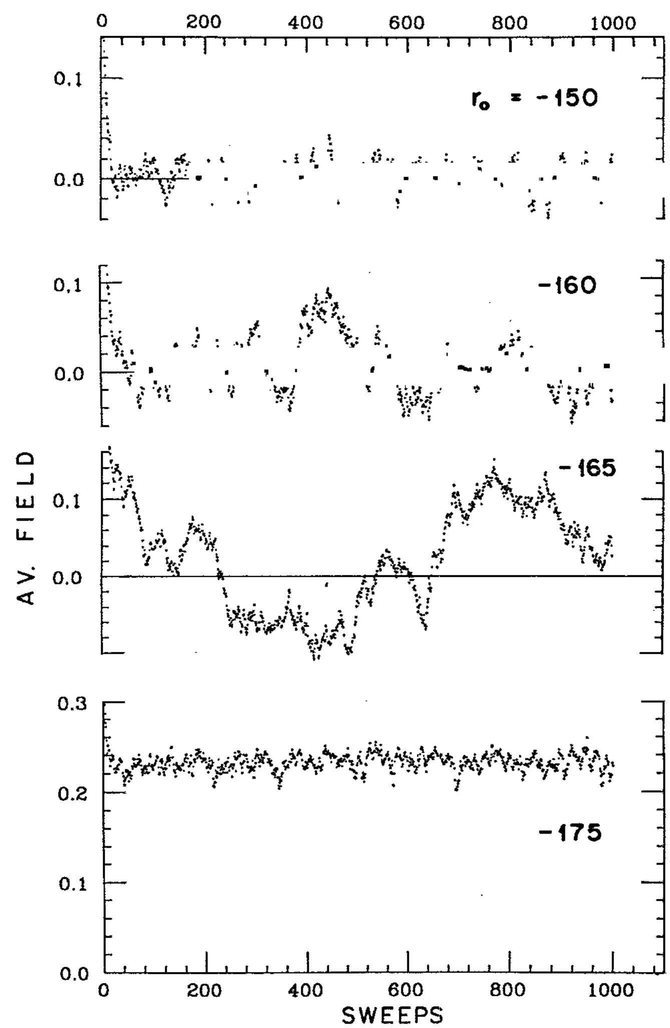

FIG. 1. Evolution of the field. The field averaged over the lattice is shown for 1000 successive Monte Carlo sweeps of the lattice, for $\lambda_0=1000$ and various values of r_0. In the initial configuration the field was 0.35 at all sites.

The computations were done on a VAX 780. Typically it took 200 sweeps to warm up the lattice. For the case $J=0$, 10 000—20 000 sweeps were needed to obtain an acceptable level of accuracy for the propagator. Generating an acceptable effective potential is easier, requiring only 2000—5000 sweeps, depending on how close we were to the critical point. The CPU time required was about 1 day for 10 000 sweeps. At this rate a calculation of λ_r via the 4-point function would be practically impossible, due to the large errors introduced by the subtractions required for connected parts. On the other hand, calculating the effective potential proves to be a very efficient and economical way to obtain both λ_r and $m_{\rm latt}$.

Because of the finite size of the lattice, there is no sharp phase transition, and $m_{\rm latt}$ never actually goes to zero. To help determine the critical point as best we could, we kept a record of the average field over the lattice, at successive sweeps. That is, we kept track of the evolution of the average field. In this manner, we could see in detail how spontaneous symmetry breaking develops when r_0 was varied across the critical point. Some samples are shown in Fig. 1 for the case $\lambda_0=1000$. For $r_0=-150$ the average field makes small fluctuations about zero. The fluctuations become more pronounced as r_0 is decreased toward the critical point between -160 and -165. Spontaneous symmetry breaking is already evident at -165, where the field flip-flops with a period much greater than the characteristic time scale at -160. By -175 the period has become much greater than the observation time, and broken symmetry becomes manifest on a macroscopic scale.

III. RESULTS AND DISCUSSIONS

We have carried out computations for $\lambda_0=1$, 100, 1000, ∞. The first value is small enough to allow a comparison with perturbation theory, and the last limiting value corresponds to the 4D Ising model. Figure 2 shows plots of the derivative of the effective potential for $\lambda_0=1$, for a range of values of r_0 that includes the critical point. Figure 3 shows various parameters as functions of r_0, for $\lambda_0=1$. In both figures the predictions of zero-loop and one-loop perturbation theories are also shown for comparison. Figures 4 and 5 give the same plots for $\lambda_0=100$, but comparison with perturbation theory for this case is inappropriate, and therefore omitted.

The data for Z in Figs. 3 and 5 are obtained from the effective potential. The corresponding data obtained from the propagator via (4) are consistent with the above in the symmetric phase, both in central values and statistical errors. In the "broken" phase, however, the data obtained via the propagator have such large errors as to render them useless. This demonstrates the efficacy of the effective potential method.

In the weak-coupling case $\lambda_0=1$, the predictions of one-loop perturbation theory compare well with the numerical results away from the critical point, but they break down near the critical point. For example, perturbation theory yields a complex effective potential, whereas the actual effective potential is always real. The one-loop perturbation theory completely fails in its prediction $Z=1$. As we can see in the figures, Z depends on r_0, and vanishes at the critical point.

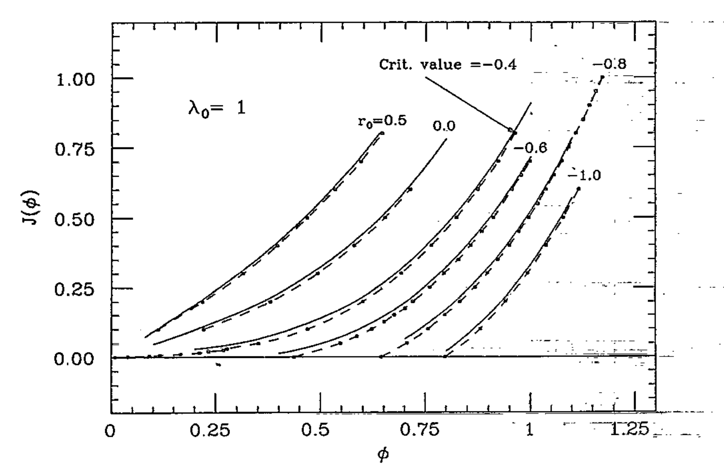

FIG. 2. Derivative of the effective potential for $\lambda_0=1$ for a range of values of r_0 that includes the critical point $r_c=-0.4$. Statistical errors are of the order of the size of the points shown. Predictions of one-loop perturbation theory are shown by the solid lines. For $r_0<r_c$ perturbation theory completely fails near $\phi=\phi_0$: it gives a complex effective potential.

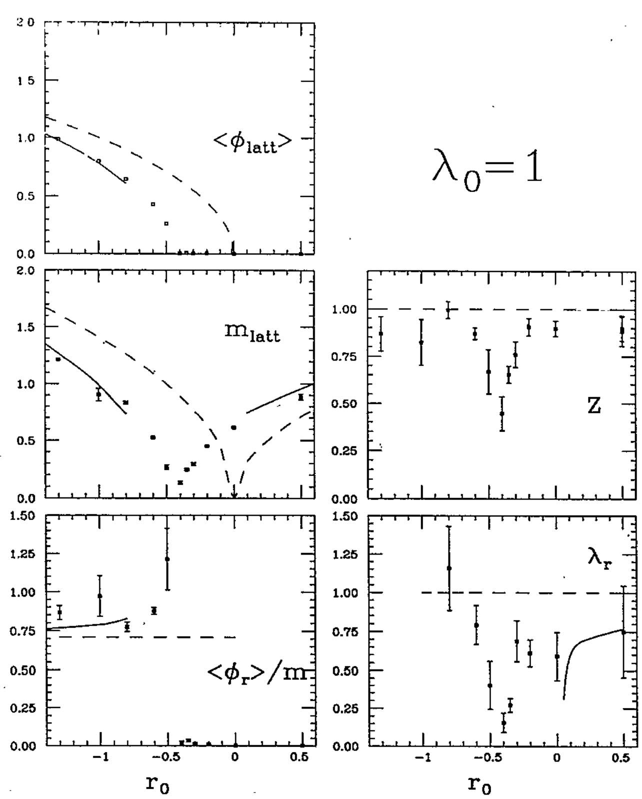

FIG. 3. The following quantities are plotted against r_0 for $\lambda_0=1$: $\langle\phi_{\rm latt}\rangle$=vacuum expectation of the field in lattice units, $m_{\rm latt}$= the mass gap in lattice units, $b=\langle\phi_r\rangle/m$ (ratio of renormalized field to physical mass gap), Z=wave-function renormalization constant, λ_r=renormalized self-coupling constant. Also shown are predictions of the zero-loop (dashed lines) and one-loop (solid lines) perturbation theory. Note that b is discontinuous at the critical point, while $\phi_{\rm latt}$ is continuous.

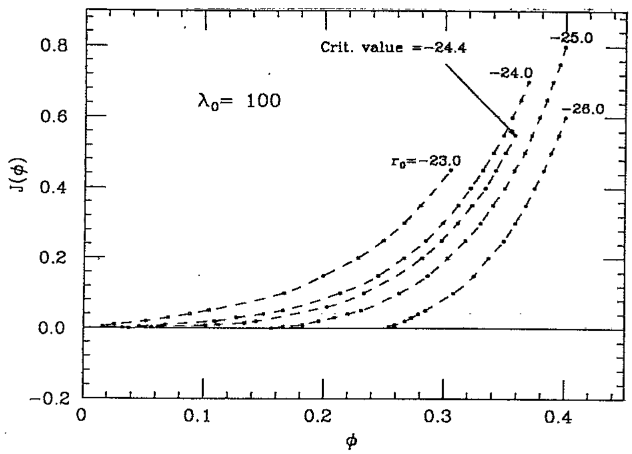

FIG. 4. Same as Fig. 2, but for $\lambda_0 = 100$. Perturbative results are not included because they are not applicable.

From the plots in Figs. 3 and 5 we see that $\langle \phi_{\text{latt}} \rangle$ and m_{latt} both vanish at the critical point, but the ratio b is discontinuous, approaching zero from one side, and nonzero from the other. This defines the two phases of the system in the continuum limit, a symmetric and a symmetry-broken phase. We shall return shortly for a closer look at the behavior of b in the symmetry-broken phase.

In Fig. 6 we plot the renormalized coupling λ_r as a function of m_{latt}, for various values of the unrenormalized coupling λ_0. The origin corresponds to the continuum limit. Separate plots are given for the two different phases corresponding to $r_0 > r_c$ and $r_0 < r_c$. We see that the limiting curve with $\lambda_0 = \infty$ divides the plane into two parts, and no point falls to the left of it. This clearly shows the ghost point, the smallest possible m_{latt} for fixed renormalized coupling, where the bare coupling diverges. The forbidden region is presumably ghost land, to which unfortunately computers are still denied access.

Figure 7 shows results for the three-particle vertex in the symmetry-broken phase. This parameter is proportional to λ_r in lowest-order perturbation theory, but in general it might be an independent quantity. Here we check that it indeed vanishes in the continuum limit as expected, thus explicitly demonstrating that in the continuum limit there is neither three-particle nor four-particle vertex.

The boundary of the forbidden region in Fig. 6 is the locus of the ghost point corresponding to various values of λ_r. These values, the closest possible approach to the continuum limit for a given $\lambda_r > 0$, are larger from those predicted by perturbation theory in (12) by orders of magnitude. That is, on the scale of Fig. 6, perturbation theory would have λ_r drop to zero precipitously near the contin-

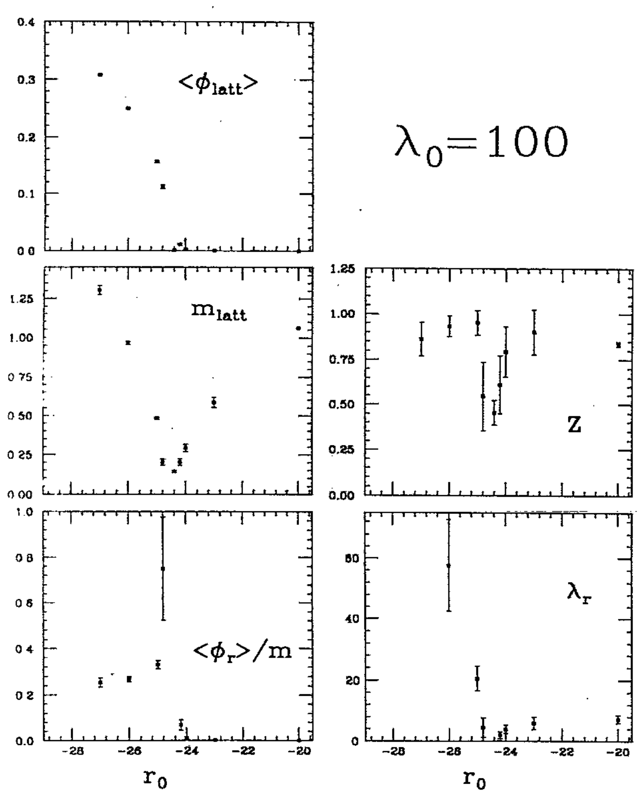

FIG. 5. Same as Fig. 3, but for $\lambda_0 = 100$.

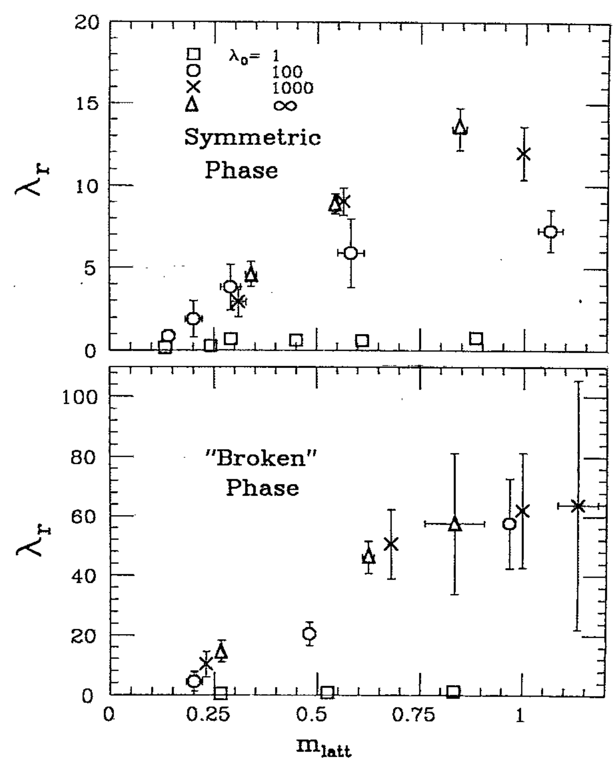

FIG. 6. The renormalized coupling λ_r as a function of m_{latt}, which is proportional to the lattice spacing. The family of data points refers to different values of the bare coupling: $\lambda_0 = 1$, 100, 1000, ∞. The limiting case $r_0 = \infty$ corresponds to the 4D Ising model. At fixed λ_r, the lattice spacing cannot be made smaller than a minimum number, the ghost point (at which a ghost state presumably appears). The only way to reach the continuum limit is to "slide down" the limiting Ising curve (or any curve in the region below it) toward $\lambda_r = 0$. Ninety percent of the errors in the data come from uncertainties in the extraction of m_{latt} or Z from the propagator.

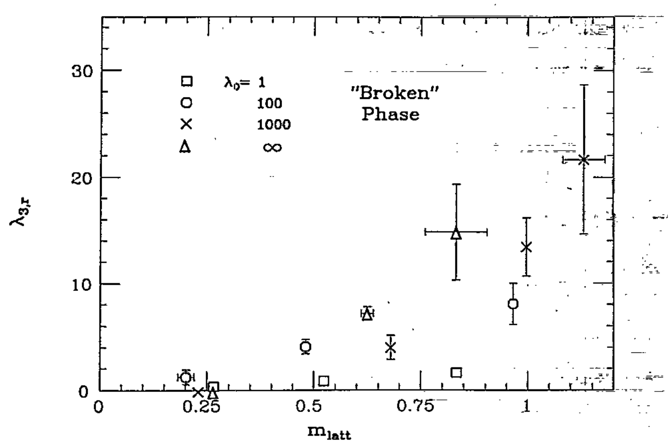

FIG. 7. The renormalized three-particle vertex in the symmetry-broken phase, in plots similar to those of Fig. 6 for the four-particle vertex.

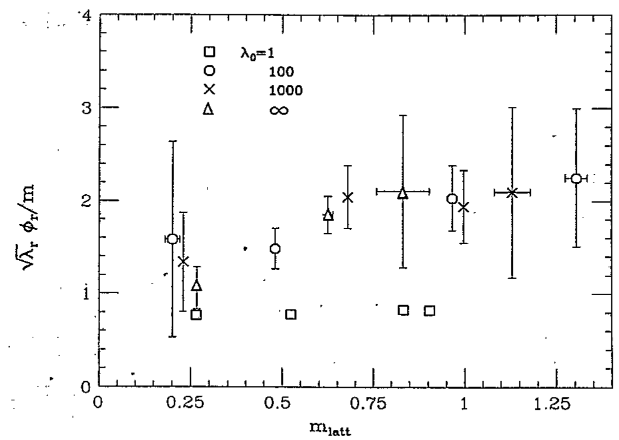

FIG. 9. Perturbation theory predicts that the quantity plotted approaches a constant independent of λ_0 in the continuum limit. The data seem to be at variance with that prediction.

uum limit. Instead, our results show a gentle decrease. The reason is that the vanishing of λ_r in Fig. 6 is caused mainly by the fact that $Z \to 0$, whereas perturbation theory, even with the summing of all one-loop graphs, gives $Z = 1$.

In the present theory the value of the parameter b is without physical significance. Nevertheless we shall examine it in greater detail, for it may give an indication of whether the Higgs mechanism still works when the scalar field is coupled to other fields, despite the fact that $\lambda_r = 0$. To this end we exhibit b in Fig. 8 as a function of $m_{\rm latt}$ in the symmetry-broken phase, for various values of λ_0. It appears that b extrapolates to different values in the continuum limit, depending on λ_0. This would indicate that the vacuum expectation of the field sets an arbitrary mass scale independent of m.

However, the numerical data cannot rule out the possibility that b diverges in the continuum limit—an expected behavior if one believes in the relation $b \propto \lambda_r^{-1/2}$ from perturbation theory. To test this, we plot $\lambda^{1/2} b$ as a function of $m_{\rm latt}$ in Fig. 9, for various values of λ_0. The function is remarkably constant for $\lambda_0 = 1$; but for larger values of λ_0 it appears to approach zero in the continuum limit. We take this to be tentative indication that b is a parameter independent of λ_r and that λ_0 is not an irrelevant parameter of the theory.

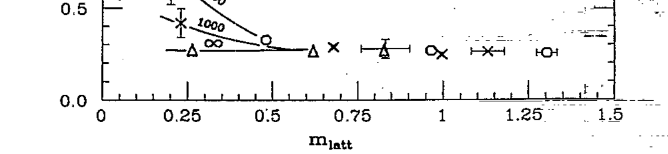

FIG. 8. Dimensionless ratio between the vacuum field and the renormalized mass as a function of $m_{\rm latt}$, which is proportional to the lattice spacing. The solid lines are free-hand drawings to guide the eye.

IV. CONCLUSION

The existence of a phase in the continuum limit with broken symmetry suggests that, even though the renormalized self-coupling is zero, a gauge field coupled to the scalar field can acquire mass through the usual Higgs mechanism. In fact Coleman and Weinberg[8] have verified this in perturbation theory. The answer is by no means certain, however, because the self-consistency of the perturbative treatment relies on the implicit assumption $\lambda_r > 0$, which is not true.

The question of generating fermion masses remains equally open. If we couple a fermion to the scalar field through the Yukawa coupling $g\bar{\psi}\phi\psi$ we might expect to generate a mass term $g_r \langle\phi\rangle\bar{\psi}\psi$. But the renormalized Yukawa coupling g_r may vanish in the continuum limit, since it is not asymptotically free. Then, again, this may be compensated by the fact that b actually diverges. On top of all the uncertainty, we must add the further caveat that the mass term above is no more than a naive expectation suggested by perturbation theory.

In closing we must draw particular attention to the fact that the resulting field theory in the continuum limit is drastically different from what we have been conditioned to expect by perturbation theory. In the phase with broken symmetry, the "Higgs"-boson mass m is arbitrary, even though $\lambda_r = 0$. Perturbation theory would have us erroneously believe that m is proportional to $\lambda_r^{1/2}$. The lesson we learn is that it is futile to make conjectures on generating masses for gauge fields and fermions. First of all, the perturbative connection between coupling constants and masses may not hold. Second, introducing new couplings may drastically change the system. These physically relevant problems will have to be studied by nonperturbative methods and we are continuing our computational program to address them.

ACKNOWLEDGMENTS

We thank J. Shigemitsu for pointing out an error in the original handling of the data in Fig. 6. This work was supported in part by funds provided by the U.S. Department of Energy (D.O.E.) under Contract No. DE-AC02-76ER03069.

*On leave from the Central Research Institute for Physics, Hungarian Academy of Sciences, Budapest, Hungary.

[1]See K. G. Wilson, Rev. Mod. Phys. **55**, 583 (1983), for summary and literature.

[2]B. Freedman, P. Smolinsky, and D. Weingarten, Phys. Lett. **113B**, 481 (1982).

[3]Following are sources of literature. For analytical studies see J. Frohlich, Nucl. Phys. **B200**, 281 (1982). For numerical studies see C. B. Lang, *ibid.* **B265**, 630 (1986).

[4]See K. Huang, *Quarks, Leptons, and Gauge Fields* (World Scientific, Singapore, 1982), Chap. 10, for a general discussion of the effective potential.

[5]T. D. Lee, Phys. Rev. **95**, 1329 (1954).

[6]G. Källén and W. Pauli, K. Dan. Vidensk. Selsk. Mat. Fys. Medd. **30**, No. 7 (1955).

[7]See Huang, *Quarks, Leptons, and Gauge Fields* (Ref. 4), Chap. 9.

[8]S. Coleman and E. Weinberg, Phys. Rev. D **7**, 1888 (1973).